# JACS

# Direct Modulation of Microtubule Stability Contributes to Anthracene General Anesthesia

Daniel J. Emerson,[†,§] Brian P. Weiser,[‡,§] John Psonis,[†] Zhengzheng Liao,[†] Olena Taratula,[†] Ashley Fiamengo,[†] Xiaozhao Wang,[†] Keizo Sugasawa,[†] Amos B. Smith, III,[†] Roderic G. Eckenhoff,*[‡] and Ivan J. Dmochowski*[†]

[†]Department of Chemistry, University of Pennsylvania, 231 South 34th Street, Philadelphia, Pennsylvania 19104, United States

[‡]Department of Anesthesiology & Critical Care, Perelman School of Medicine, University of Pennsylvania, 311A John Morgan Building, 3620 Hamilton Walk, Philadelphia, Pennsylvania 19104, United States

ⓢ Supporting Information

**ABSTRACT:** Recently, we identified 1-aminoanthracene as a fluorescent general anesthetic. To investigate the mechanism of action, a photoactive analogue, 1-azidoanthracene, was synthesized. Administration of 1-azidoanthracene to albino stage 40−47 tadpoles was found to immobilize animals upon near-UV irradiation of the forebrain region. The immobilization was often reversible, but it was characterized by a longer duration consistent with covalent attachment of the ligand to functionally important targets. IEF/SDS-PAGE examination of irradiated tadpole brain homogenate revealed labeled protein, identified by mass spectrometry as $\beta$-tubulin. In vitro assays with aminoanthracene-cross-linked tubulin indicated inhibition of microtubule polymerization, similar to colchicine. Tandem mass spectrometry confirmed anthracene binding near the colchicine site. Stage 40−47 tadpoles were also incubated 1 h with microtubule stabilizing agents, epothilone D or discodermolide, followed by dosing with 1-aminoanthracene. The effective concentration of 1-aminoanthracene required to immobilize the tadpoles was significantly increased in the presence of either microtubule stabilizing agent. Epothilone D similarly mitigated the effects of a clinical neurosteroid general anesthetic, allopregnanolone, believed to occupy the colchicine site in tubulin. We conclude that neuronal microtubules are "on-pathway" targets for anthracene general anesthetics and may also represent functional targets for some neurosteroid general anesthetics.
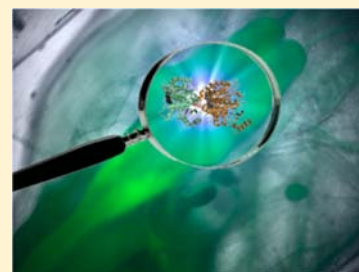
## INTRODUCTION

For 170 years general anesthetics (starting with diethyl ether) have been administered to human patients, who are rendered nonresponsive to painful medical procedures. To this date, surprisingly little is known about the relevant anesthetic targets, which has compromised the development of not only more potent but also safer anesthetic drugs. Current hypotheses of anesthetic action invoke specific ligand−protein interactions.[1] However, anesthetic drugs display only modest affinity for the putative targets as well as many proteins subserving "off-pathway" (undesirable) effects.[2−4] A wide range of life forms, including plants, are influenced by general anesthetics, which suggests common protein targets that are evolutionarily conserved. The different pharmacology and chemical diversity of anesthetic drugs also suggests that in humans there are multiple routes to achieving the same anesthetic end point. Still lacking are validated, relevant targets, as well as knowledge of their in vivo distribution. The development of anesthetic probe molecules provides a route to address these challenges.[5] The ability to identify general anesthetic protein targets and binding sites has been enhanced with anesthetic photolabels containing diazo or azido functional groups.[6−11] Carbene or nitrene intermediates can be generated with absorption of long-wavelength ultraviolet light (315−400 nm), enabling ligand

attachment onto physiologically relevant sites on cellular macromolecules, when equilibrated prior to photolysis. The covalently linked photolabel provides a tag identifiable with mass spectrometry; however, radiolabeled versions of these probes have often been essential to novel target discovery and/or binding site identification with Edman degradation.[12,13]

Previously, our laboratories identified 1-aminoanthracene (1-AMA) as a GABAergic fluorescent general anesthetic that reversibly induces immobility in *Xenopus laevis* tadpoles.[14] Using confocal laser scanning microscopy, 1-AMA was found to localize to the central nervous system (CNS).[14,15] The efficacy of 1-AMA as an anesthetic, combined with optical and biochemical advantages of fluorescent probes over radiolabels, prompted us to investigate the protein targets. To facilitate target identification, we synthesized a photoactive analogue, 1-azidoanthracene (1-AZA), by replacement of the amino group with an azide. We demonstrated that 1-AZA shares conserved anesthetic targets in tadpoles through targeted in vivo photolabeling, which produces an anesthetic-like state reminiscent of optoanesthesia,[16] a light-induced "prolongation" of the anesthetic state mediated by covalent occupation of relevant

ligand binding sites. The anthracenes 1-AMA and 1-AZA display binding specificity for neuronal tubulin and the disruption of microtubule dynamics in vitro. Finally, we have identified 1-AZA binding sites on tubulin with mass spectrometry and provided in vivo evidence that microtubule destabilization contributes to 1-AMA "anesthesia".

## ■ EXPERIMENTAL SECTION

**Spectroscopy, Chromatography, and Fluorescence Microscopy.** ^{1}H NMR (500 MHz) and ^{13}C NMR (125 MHz) spectra were obtained at room temperature in CDCl$_3$ on Bruker DMX 500 spectrometers. Spectra were referenced to the central line of the solvent residual, and the chemical shifts ($\delta$) are reported to a precision of $\pm 0.01$ and $\pm 0.1$ ppm for ^{1}H and ^{13}C, respectively. Proton coupling constants ($J$) are reported in Hz to a precision of $\pm 0.1$ Hz. High-resolution mass spectra (HRMS) were obtained using electrospray ionization with a Micromass Autospec. An Agilent Technologies 8453 spectrophotometer with temperature controller (89090A) was used for UV−vis spectroscopy with a quartz cuvette (1 cm path length), and a Varian Cary Eclipse instrument was used for fluorescence spectroscopy.

Silica gel with 60 Å pore size and 40−75 mm particle size (Sorbent Technologies) was used for column chromatography, and thin-layer chromatography was performed using silica gel plates with 60 Å pore size (Whatman) with 254 nm for detection.

Fluorescence experiments were performed with an Olympus Fluoview FV1000 confocal laser scanning microscope equipped with an inverted IX81 microscope with visible laser (488 nm Ar ion) for 1-AMA and 1-AZA imaging and near-UV lasers (351 and 364 nm, Enterprise II system) for uncaging. Tadpoles incubated with 1-AZA in pond water were irradiated with both near-UV lasers (100% power) by rastering over the forebrain using an Olympus air objective UPLSAPO 10× (NA = 0.40) with dwell time of 2 $\mu$s per pixel; after 20 s had elapsed all animals were immobilized. Images for Figure 1 were collected with a hyperspectral CCD (CRi Nuance FX) camera with collection window centered at 520 nm (bandwidth fwhm = 20 nm), coupled to an inverted fluorescence microscope (Olympus IX81). Samples were excited with a mercury lamp with a CFP filter set (excitation filter BP400-440, dichroic mirror DM455, emission filter BA475). An Olympus air objective UPLSAPO 4× (NA = 0.16) was used to collect images.

**Synthesis of 1-Azidoanthracene (2).** A solution of sodium nitrite (0.088 mg, 1.3 mmol, 1.2 equiv) in water (0.5 mL) was added dropwise at 0 °C over 10 min to a solution of 1-AMA (**1**) (0.201 mg, 1.04 mmol, 1.0 equiv) dissolved in 20% HCl (3 mL), following Scheme 1. The reaction mixture was stirred at 0 °C for 30 min before

**Scheme 1. Conversion of 1-Aminoanthracene (1-AMA, 1) to 1-Azidoanthracene (1-AZA, 2)**
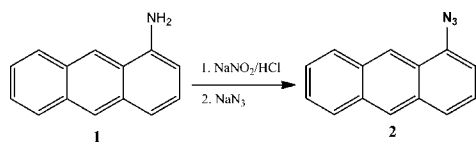


sodium azide (0.085 g, 1.3 mmol, 1.2 equiv) in water (0.5 mL) was added dropwise over 10 min. The solution was slowly warmed to room temperature and stirred for 4 h. Extraction with diethyl ether gave the crude product as brown solid, which was purified by silica gel flash column chromatography (hexane:CH$_2$Cl$_2$, 20:80, v/v) to yield 0.081 g (0.37 mmol, 35% yield) of **2** as a red solid. Thin layer chromatography (silica gel, hexane:CH$_2$Cl$_2$, 20:80, v/v): $R_{f(2)}$ = 0.9. ^{1}H NMR: $\delta$ 8.67 (s, 1H), 8.40 (s, 1H), 8.03 (m, 2H), 7.80 (d, $J$ = 8.5 Hz, 1H), 7.44−7.51 (m, 3H), 7.23 (d, $J$ = 7.1 Hz, 1H). ^{13}C NMR: $\delta$ 136.9, 132.4, 131.8, 128.9, 128.2, 126.4, 126.3, 125.9, 125.4, 125.2, 124.9, 121.8, 112.9.

**Localized in Vivo Photolabeling.** For 1-AZA labeling studies, stage 40−47 albino *Xenopus laevis* tadpoles (Nasco, Fort Atkinson,

WI) were incubated for 30 min in 5 mL of pond water (3.15 mM CaCl$_2$, 30.36 mM NaCl, and 0.59 mM NaHCO$_3$ in deionized water) with 0.5% ethanol containing 15 $\mu$M 1-AZA. Tadpoles were briefly washed with fresh water and directed into a Delta T culture dish (Bioptechs). The Delta T culture dish consisted of a coverslip at the bottom with a tapered agarose channel (solidified 1% w/v in water) to restrict movement.

A similar protocol for tadpole incubation and UV laser exposure (except 10 s irradiation at 100% power) was followed for the fluorescence images generated for Figure S1 using an Olympus air objective UPLSAPO 10× (NA = 0.40). Anthracene fluorescence emission was collected by confocal microscopy in 500−600 nm range under excitation of 488 nm laser at scanning speed of 2.1 s/frame. The images were processed with ImageJ software to get the averaged pixel intensity in the region of interest (ROI).

In quantifying anesthetic end points, individual tadpoles were incubated with corresponding concentrations of 1-AMA or 1-AZA for 30 min in 5 mL of pond water after 1-h incubation in 2 $\mu$M epothilone D (EpoD) or vehicle. Alternatively, tadpoles were pre-incubated with 2 $\mu$M discodermolide (disco). Pond water samples were then assayed by UV−vis spectroscopy to determine 1-AZA and 1-AMA concentrations. Subsequently, each tadpole was placed in 5 mL of fresh pond water to assess anesthetic end points. Tadpoles scored as "immobile" did not swim, twitch, or right themselves for 30 s, nor did they respond to a gentle tail stroke manually administered with the blunt end of a sterile cotton swab. For the purposes of this work, "anesthesia" is hereafter defined as reversible immobility. Death was determined by cessation of heartbeat, visible by microscope through the transparent organism.

**Induction Assay: 1-AMA.** Ten tadpoles per dish were equilibrated with 1-AMA (5−60 $\mu$M) for 30 min before assessing immobility as described above. The pond water contained 0.5% ethanol for 1-AMA solutions below 30 $\mu$M and 1% ethanol above 30 $\mu$M. For some experiments, tadpoles were incubated with 2 $\mu$M EpoD for 1 h before addition of 1-AMA. Pond water samples were assayed by UV−vis spectroscopy immediately after experiments to ensure soluble 1-AMA concentrations were maintained. The tadpoles were then placed into fresh pond water for recovery.

**Induction Assay: Allopregnanolone.** For comparison with 1-AMA, 9−11 tadpoles per dish were equilibrated with the neurosteroid allopregnanolone (3$\alpha$-hydroxy-5$\alpha$-pregnan-20-one) for 3 h in pond water containing 0.5% ethanol, following the protocol of Wittmer et al.[17] Allopregnanolone (3 or 4 $\mu$M in pond water) was added from a 6 mM stock solution in DMSO such that DMSO volume was negligible (<0.06%). Tadpoles were transferred to fresh allopregnanolone solution after 1.5 h, to ensure a stable anesthetic concentration. Tadpole immobilization was monitored and recorded during 3 h induction. Subsequently, recovery was observed after switching to pond water.

**Western Blotting.** Tadpoles were treated with 60 $\mu$M 1-AMA in pond water for 30 min with or without prior incubation with 2 $\mu$M EpoD for 1 h (similar to the Induction Assay method, except here 15 tadpoles were used for each treatment). After treatment, the dishes containing the tadpoles were placed on ice. Individually, the brains were removed with forceps under a dissecting microscope after decapitation behind the hindbrain. Tissue was placed directly in 20 mM Tris buffer, pH 7.6, 5% glycerol, 1% Triton X-100, and 0.5% SDS supplemented with protease inhibitors; after homogenization the samples were frozen at −80 °C. The two groups of tadpoles (±EpoD) were treated with the same stock of 1-AMA, but not simultaneously to ensure timely removal of neuronal tissue following treatment. Less than 5 min was required to isolate tissue from each group following the 30 min 1-AMA equilibration.

After thawing, the insoluble pellets were removed by centrifugation, and a protein assay was performed on the supernatants containing solubilized neuronal protein. Protein was separated by SDS-PAGE and transferred to PVDF. After blocking with 1.5% (w/v) bovine serum albumin dissolved in TBS-T (Tris-buffered saline with 0.1% Tween-20), primary antibodies (in TBS-T at a 1:1000 dilution) were applied overnight at 4 °C. Primary antibodies were from Sigma-Aldrich (anti-tyrosine tubulin-$\alpha$, clone TUB-1A2, catalog no. T9028 and anti-

acetylated tubulin-α, clone 6-11B-1, catalog no. T7451). A secondary antibody conjugated to horseradish peroxidase was applied for 1 h in TBS-T before developing the blots with Amersham ECL Select reagent and a Kodak Image Station 4000 MM Pro. The membranes were subsequently washed in water, stained with Coomassie R-250, and scanned with a Bio-Rad GS-800 calibrated densitometer.

**In Vitro Tadpole Photolabeling.** Following tricaine methanesulfonate anesthesia, tadpoles were dissected with brains isolated, homogenized in sucrose isolation buffer, and washed as described.[16] Photolabeling of the isolated neuronal membranes proceeded with an oversaturated solution of 1-AZA (∼200 μM). After 5-min incubation in the dark, the homogenate was photolabeled for 1 min in a quartz cuvette (path length 1 mm) with a 12 in. × 12 in. tabletop Spectroline ultraviolet transilluminator (Spectronics Corp., TL-365R, 9 mW/cm$^2$ at peak intensity, 365 nm). The duration of UV illumination required for complete 1-AZA photodissociation was determined to be 25 s through separate experiments. The photolabeled membranes were washed and prepared for IEF/SDS-PAGE as described;[16] a Bio-Rad 3−10 nonlinear pH gradient strip was used in the first dimension, with a 4−15% polyacrylamide gel in the second dimension. After separation, the gel was washed with water and scanned with a Kodak Image Station 4000 MM Pro with 400 nm excitation and 535 nm emission filters. The gel was subsequently stained with Coomassie G-250 and reimaged. Spots excised from the gel were analyzed with LC-MS/MS, as described below.

**Polymerization Assay.** Bovine tubulin (>99% purity) purchased from Cytoskeleton, Inc. (Denver, CO) was resuspended in ice-cold 1× BRB80 buffer (1 mM MgCl$_2$, 1 mM EGTA, 80 mM PIPES, pH 6.9) at 6 mg/mL, and aliquots were snap frozen in liquid nitrogen. As needed, these were thawed on ice and diluted to achieve final concentrations of 1× BRB80, 10% glycerol, 1.7% DMSO, 10.9 μM tubulin, and 14 μM test compound (colchicine, 1-AMA, or 1-AZA). In some 1-AZA experiments, this mixture was initially irradiated for 20 s using the UV transilluminator. The mixed reagents were added to a cuvette that was temperature controlled at 37 °C. This was blanked, and GTP was added to achieve a final concentration of 2 mM. Absorbance was recorded at 450 nm in order to avoid potential absorption from colchicine, 1-AZA, and 1-AMA (Figures S2 and S3).

**LC-MS/MS and Labeling Identification.** Following IEF/SDS-PAGE and staining, spots excised from the tadpole neuronal gel were trypsin digested and processed by nanoLC-MS/MS with a Thermo LTQ linear ion trap. Raw data were acquired with Xcalibur, and Sequest was used to search b and y ions from a *Xenopus* protein sequence database[16] downloaded from the National Center for Biotechnology Information web site. Search parameters were 1.5 amu parent ion mass tolerance, 1 amu fragment ion mass tolerance, and 1 missed cleavage. Cysteine carbamidomethylation and methionine oxidation were permitted as variable modifications, and search result files were filtered with the following criteria: 99.9% protein identification confidence with 2 peptide minimum, and peptide Xcorr scores of (+1 ion) 1.7, (+2 ion) 2.3, or (+3 ion) 2.8.

In addition, bovine tubulin (from Cytoskeleton, Inc.) was used for mass spectrometry sequencing experiments. The protein was incubated with an oversaturated 1-AZA solution (200 μM) for 20 min under polymerizing conditions (see Polymerization Assay method) before irradiating with the UV transilluminator for 1 min. SDS was added to the solution, and covalent attachment was confirmed via fluorescence after SDS-PAGE by scanning the gel. After Coomassie staining, the ∼50 kDa monomer band was excised for analysis. Samples were processed as above, but spectra were searched against a database composed of 13 *B. taurus* tubulin isoforms (six α- and seven β-tubulin sequences). Search parameters and filters described above were used, but with the additional permission of a variable 191.24 amu modification on each amino acid (corresponding to a 1-AZA photolabel adduct). High-scoring spectra were manually inspected to ensure quality and confidence.

**Anthracene−Colchicine Competition.** For 1-AZA experiments, 15 μM tubulin (prepared from snap frozen aliquots in the same procedure as the polymerization assay) was incubated for 10 min in 1× BRB80 with 8 μM 1-AZA and 50 μM colchicine at 4 °C. Irradiation

with the near-UV transilluminator then proceeded for 1.5 min to ensure complete 1-AZA photolysis. Fluorescence spectra were recorded with 425 nm excitation in order to avoid the potential for competing absorption from colchicine. For 1-AMA experiments, 100 μM tubulin in 1× BRB80 was incubated with 50 μM 1-AMA for 10 min before varying colchicine concentrations were added at 4 °C. Tubulin was maintained in the depolymerized state for both 1-AZA and 1-AMA experiments. Binding/covalent labeling was monitored by fluorescence intensity at 4 °C. The fluorimeter PMT was set to 800 V, with excitation and emission slit widths of 5 nm. The peak for 1-AZA corresponding to labeled tubulin was recorded at 500 nm and around 520 nm for 1-AMA. Upon colchicine addition, loss of binding was seen with 1-AMA (intensity reduction with red-shifted emission). When 1-AZA was titrated into tubulin pre-incubated with colchicine, loss of labeling was also seen through signal reduction.

In addition to fluorescence, a denaturing gel was used to confirm colchicine/1-AZA competition. Three 30 μL samples of 16 μM tubulin were incubated for 35 min at 4 °C in 1× BRB80 and 1.5% DMSO with and without the presence of 20 mM colchicine (colchicine stock solution of 1.3 M dissolved in DMSO). Afterward, 9 μM 1-AZA was added (1-AZA stock solution of 1.8 mM dissolved in ethanol) to one tubulin sample with colchicine and another without colchicine. Then, all three samples (1-AZA alone, colchicine alone, and 1-AZA plus colchicine) were photolyzed with transilluminator for 2 min. Loading buffer (10 μL of 4× SDS-PAGE) was added to each sample, and SDS-PAGE was then performed.

**Figures, Calculations, and Statistics.** Graphical figures were created with Gnuplot 4.2 and GraphPad Prism 6.0. Protein structural images were created with PyMOL using data deposited in the PDB.[18] The tadpole dose−response curve was generated within Prism software, fitting a sigmoidal curve with variable slope to the equation:

$$y = \frac{100}{1 + (10^{\log EC_{50}-x})n}$$

where $n$ is the Hill slope. $n = 5.4 \pm 2.7$ for 1-AMA with EpoD and 4.4 $\pm$ 1.1 for 1-AMA alone. $EC_{50} = 16$ μM $\pm$ 0.5 μM for 1-AMA with EpoD and 8 μM $\pm$ 0.5 μM for 1-AMA alone (best-fit value ±95% confidence interval).

The maximum rate, $V_{max}$, of tubulin polymerization was determined for tubulin alone and in the presence of colchicine, 1-AZA ($\pm$ UV), 1-AMA, and other anesthetics. $V_{max}$ was calculated from the initial slope of the increasing absorbance at 450 nm after the first minute, when increase in scattering occurred due to mixing: $V_{max} = \Delta Abs_{450} \times 1000/$min (mOD/min).[19]

For allopregnanolone-EpoD competition experiments in tadpoles, a $t$ test "two sample assuming unequal variances" was performed using Data Analysis Tools in Microsoft Excel 2007.

# ■ RESULTS

**Synthesis and Characterization.** 1-AZA was synthesized from 1-AMA in two steps, purified by column chromatography and isolated in 35% yield (Scheme 1) with modifications to a published protocol.[20] Replacement of the amine with an azide increased the molecular weight of the otherwise isostructural compound by 26 Da. The UV−vis spectrum of 1-AZA displays a pronounced triple absorption peak ($\lambda_{abs} = 350−400$ nm), corresponding to the azido moiety (Figure S2b), and an extinction coefficient was determined at 372 nm: $\varepsilon_{372} = 9100$ M$^{-1}$ cm$^{-1}$. Complete photolysis of the azide via UV transilluminator or near-UV laser exposure occurred rapidly, consistent with previous studies on aryl azides,[21] with the transient product containing a reactive nitrene[12] capable of protein attachment.[20] The chemistry of aryl azides as protein photolabels has been extensively investigated.[22] At tested concentrations, 1-AZA was found to be ineffective as a tadpole immobilizer. However, upon 1-AZA photolysis in the forebrain, many tadpoles were reversibly immobilized; global photolysis
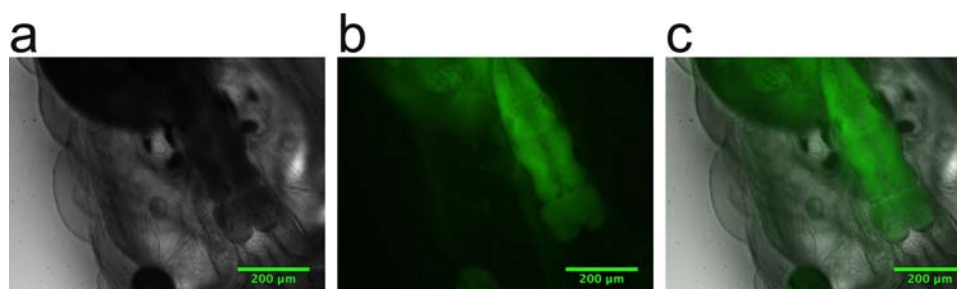
**Figure 1.** Confocal microscopy of 1-AZA-labeled tadpoles. (a) Bright-field image (4× magnification) of tadpole brain with 15 μM 1-AZA. (b) 4× fluorescent image of tadpole brain with 15 μM 1-AZA. (c) Overlay of fluorescent and bright-field images. Scale bar = 200 μm.

of 1-AZA revealed a similar fluorescence distribution profile to the parent anesthetic in the CNS (Figure 1). As a measure of specific binding, average fluorescence intensity in the forebrain relative to the area between forebrain and eye was quantified for 1-AZA, 3.2 ± 0.8 ($n$ = 7), and 1-AMA, 5.6 ± 1.8 ($n$ = 5). The amino group of 1-AMA hydrogen-bonds with water; replacement increases the hydrophobicity of the anthracene (calculated[23] LogP of 1-AZA = 5.4, of 1-AMA = 3.7). This results in low water solubility at pH 7 (1-AZA, 7 ± 3 μM; 1-AMA, ∼33 μM), which would significantly reduce target site occupancy assuming that 1-AZA and 1-AMA have similar binding affinity.

**In Vivo and In Vitro Photolabeling.** Our recent work demonstrated that covalent attachment of equilibrated anesthetic photolabel (*meta*-azi-propofol[10] [aziP*m*]) in vivo transforms low affinity binding to a long-term, functionally relevant interaction.[16] As with aziP*m*, we hypothesized that covalent attachment of the ligand at sub-anesthetic doses in vivo would result in anesthesia by enhancing occupancy by 1-AZA at molecular sites of action. Using our UV confocal microscope, we photolyzed 1-AZA in the forebrain of albino tadpoles, as whole body labeling was found to be lethal, and the forebrain provided an explicit and isolable target for replicate experiments. As expected, the fluorescence intensity from 1-AZA was observed to increase by more than 50% upon photolysis within this region of interest (ROI), see Figure S1. The ability of the azide moiety to quench anthracene fluorescence through a photoinduced electron-transfer (PET) mechanism has been previously observed,[24] and as such provides a general class of 'turn-on' fluorescence reporters upon conversion of aromatic azides to the corresponding fluorophore amines.[25−29]

1-AZA (5 μM) administered with UV microscope-localized in vivo labeling was still somewhat toxic (19/35 animals did not recover), while reversible immobility occurred in >60% of the remaining 16 animals (Figure 2a and Table 1). As expected, tadpoles treated with 8 μM 1-AMA with and without localized near-UV recovered on similar time scales, due to the lack of a photoactive moiety, with complete recovery (Table 1). These tadpole experiments proved an immobility effect specific to 1-AZA photolysis, and suggested an effect attributable to in vivo photolabel attachment. Thus, we hypothesized that protein targets covalently labeled by 1-AZA may comprise conserved substrates of anthracene anesthesia and thereby contribute to the optoanesthetic state. Enriched tadpole neuronal membranes photolabeled in vitro with 1-AZA were separated by IEF/SDS-PAGE gel and scanned for fluorescence (Figure 2b). Spot 1 (∼50 kDa) was excised after Coomassie staining, and the major components were identified with mass spectrometry (LC-MS/MS) as *X. laevis* tubulin-*β* and tubulin-*α* isoforms (Table 2).
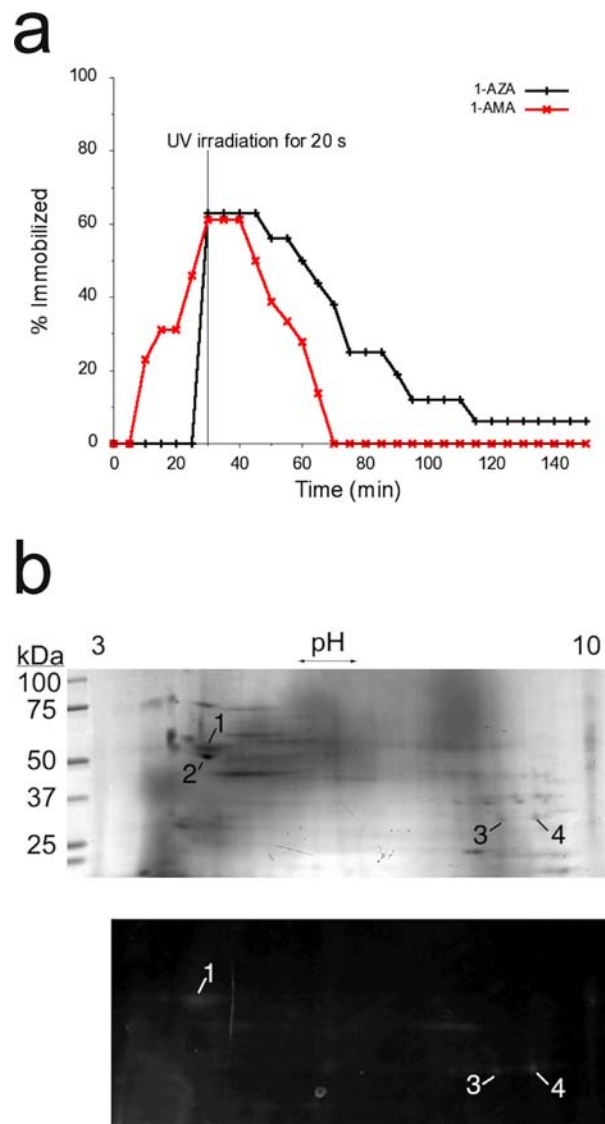


**Figure 2.** Optoanesthesia and protein labeling with 1-AZA. (a) Time course for tadpole recovery after irradiation and 30-min incubation in 1-AZA (4.6 μM ± 1.7 μM, $n$ = 16) or 1-AMA (7.5 μM ± 2.0 μM, $n$ = 13). (b) Fluorescence scan and corresponding Coomassie-stained IEF/SDS-PAGE gel of tadpole brain membranes photolabeled in vitro. Photolabeled spot 1 was identified as *X. laevis* tubulin.

Note the absence of fluorescence in spot 2, which consisted mostly of *X. laevis* ATP synthase subunit *β*, a protein with peptides also identified in spot 1. Spots 3 and 4 contained voltage-dependent anion channel 2, identified previously as a

**Table 1. Tadpole Immobilization Experiments**

| anesthetic | $n$ tadpoles | concn ($\mu$M) | % immobilized | recovery time (min) | % survival |
|---|---|---|---|---|---|
| 1-AMA | 17 | $9.7 \pm 3.7$ | 61 | $31.2 \pm 9.4$ | 100 |
| 1-AMA w/ EpoD | 18 | $9.9 \pm 5.5$ | 22 | $16.6 \pm 5.7$ | 100 |
| 1-AZA | 16 | $4.6 \pm 1.7$ | 63 | $54.5 \pm 35.4$ | 46 |
| 1-AZA w/ EpoD | 23 | $7.6 \pm 2.0$ | 34 | $41.3 \pm 19.5$ | 77 |

binding partner of other general anesthetic analogs,[16] and mass spectrometric analysis of labeled spots ~45 kDa with isoelectric points of ~7.2−7.9 yielded multiple high-confidence identifications.

**Anthracene−Tubulin Binding.** For this study, we focused on tubulin as the anthracene target, based on the large quantity of 1-AZA-labeled tubulin in all brain tissue samples tested. *X. laevis* and *Bos taurus* tubulins share ≥95% sequence homology among isoforms. To investigate anthracene-tubulin dynamics, commercially available bovine brain tubulin was used. 1-AZA was a potent inhibitor of in vitro tubulin polymerization; this effect was significantly potentiated by photo-attachment of 1-AZA, comparable to colchicine, a well-known inhibitor of tubulin polymerization.[30] The $V_{max}$ for 1-AZA together with tubulin pre-photolysis was $3.7 \pm 1.0$ mOD/min and post-photolysis was $2.0 \pm 1.5$ mOD/min, compared to that of tubulin plus colchicine, $3.1 \pm 1.0$ mOD/min. 1-AMA was less efficacious but caused significant inhibition relative to control experiments (Figure 3a). The $V_{max}$ for 1-AMA together with tubulin was $6.3 \pm 0.9$ mOD/min compared to that of tubulin control, $7.8 \pm 0.9$ mOD/min.

We next photolabeled bovine tubulin with 1-AZA and, after SDS-PAGE, identified nine tubulin isoforms with LC-MS/MS (Table S1). A search for 1-AZA conjugates identified photolabeled peptides that correspond to tubulin-$\beta 2/\beta 3$, tubulin-$\beta 5$, and tubulin-$\alpha 1D$ sequences (Figures 3b and S4a-c). The $\beta$ isoform residues are located on the S10 $\beta$ sheet, and the photolabeled tryptophan of tubulin-$\alpha 1D$ is on the H11' helix (Figures 3c and S5a-c). Structural evaluation revealed the nearest atoms on labeled/homologous residues of tubulin-$\beta 2/\beta 3$ (I368) and tubulin-$\beta 5$ (T366) as 3.3 Å and 6.7 Å,

respectively, from the nearest colchicine atoms in Ravelli et al.'s co-crystallized X-ray structure of colchicine and bovine tubulin (PDB code 1SA0).[30] Another ligand, TN16, is similarly close to these atoms, located 3.6 and 6.8 Å from the isoleucine and threonine.[31] The tubulin-$\alpha 1D$ residue is located at the interface of an $\alpha-\beta$ heterodimer, though sterically shielded from the binding pocket by the tubulin-$\beta$ H8 helix (Figure S5b). We note that the discrepancy in tubulin polymerization rate between 1-AZA pre-photolysis trial ($V_{max} = 3.7 \pm 1$ mOD/min) and 1-AMA trial ($V_{max} = 6.3 \pm 0.9$ mOD/min) might be explained by the larger log $P$ of the azide over the amine, enhancing affinity within the hydrophobic colchicine pocket.

We also photolabeled purified tubulin with 1-AZA in vitro and measured fluorescence intensity. Similar to 1-AMA,[14] photolyzed 1-AZA displayed a 4-fold increased fluorescence intensity when protein bound, and an emission maximum that shifted to 500 nm from 550 nm in water, indicative of considerable shielding from the aqueous environment. The bathochromically shifted spectrum in water results from the greater acidity of the anthracene amines in the $S_1$ state, which promotes hydrogen-bonding with solvent and decreases the energy of the $S_1 \rightarrow S_0$ transition. Excited state deactivation also results from proton donation from water.[32] Colchicine effectively protected tubulin from 1-AZA photo-attachment (Figure 3d), which was also confirmed on SDS-PAGE gel (Figure S6). Further, titration of colchicine decreased 1-AMA-tubulin binding dose-dependently (Figure 3e).

**Shifting Anesthetic Sensitivity.** Our in vitro data indicated that the anthracenes bind tubulin and decrease polymerization efficiency and/or stability. To test whether this contributes to "on-pathway" anesthetic end points, we equilibrated stage 40−47 tadpoles with 1-AMA or 1-AZA in pond water with 0.5% ethanol for 30 min after 1-h treatment with 2 $\mu$M epothilone D (EpoD), a potent microtubule stabilizing agent that binds near the taxol site.[33,34] We validated the intended pharmacologic effect in vivo with Western blot (Figures 4a and S7); acetylation of tubulin-$\alpha$ Lys40 is a surrogate marker for polymerized tubulin, while tyrosination of tubulin-$\alpha$ indicates soluble protein.[35,36] With 1-AMA, the dose−response induction curve shifted to the right with EpoD-stabilization of microtubules, increasing the 1-AMA $EC_{50}$ from

**Table 2. LC-MS/MS Protein Spot Identification**

| spot | protein ID | accession no. | MW (Da) theor[a] | MW (Da) obs[b] | pI theor[a] | pI obs[b] | spectra count | no. unique peptides |
|---|---|---|---|---|---|---|---|---|
| 1 | tubulin $\beta$-4 | gil28461386 | 49718 | 55714 | 4.82 | 5.01 | 62 | 14 |
| | ATP synth $\beta$ | gil28436792 | 56338 | | 5.25 | | 26 | 11 |
| | tubulin $\alpha$-1 | gil28422169 | 49847 | | 4.96 | | 24 | 12 |
| | tubulin $\beta$-3 | gil54311209 | 50309 | | 4.79 | | 22 | 7 |
| | tubulin $\beta$-6 | gil33417142 | 50299 | | 4.98 | | 19 | 5 |
| | tubulin $\beta$-2 | gil27696463 | 49692 | | 4.81 | | 19 | 5 |
| | tubulin $\beta$-5 | gil29124413 | 49696 | | 4.78 | | 10 | 3 |
| 2 | ATP synth $\beta$ | gil28436792 | 56338 | 51429 | 5.25 | 4.92 | 75 | 18 |
| | tubulin $\beta$-4 | gil28461386 | 49718 | | 4.82 | | 3 | 2 |
| 3 | VDAC-2 | gil62826006 | 30183 | 31750 | 8.36 | 8.59 | ref 16 | ref 16 |
| 4 | VDAC-2 | gil62826006 | 30183 | 32500 | 8.36 | 9.23 | ref 16 | ref 16 |

[a]Theoretical values calculated with ExPASy Compute pI/$M_w$ tool (http://web.expasy.org/compute_pi/). [b]Observed values calculated from the center of the spot using the molecular weight marker and IEF estimates published by the gel manufacturer.
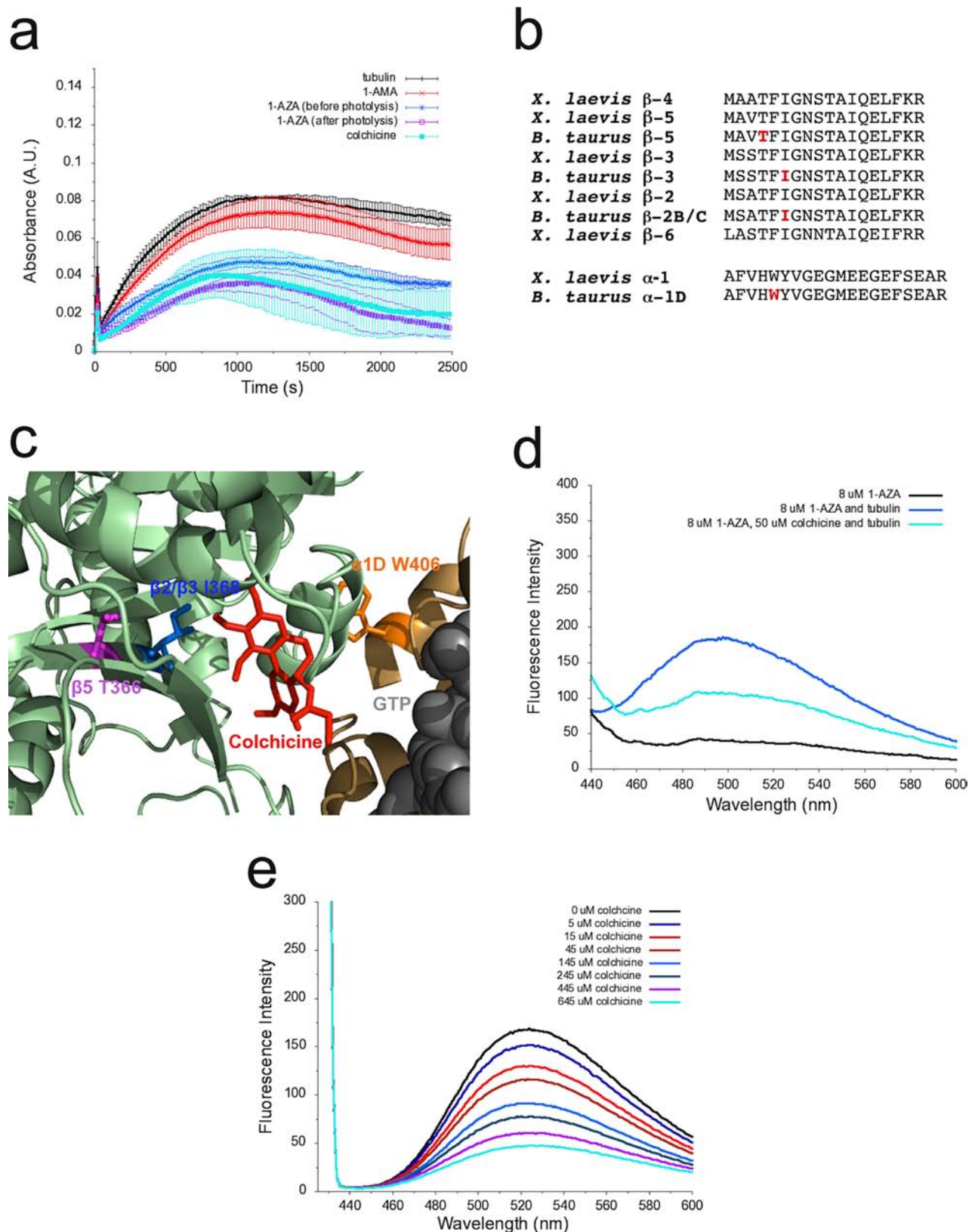
**Figure 3.** Tubulin polymerization assay and evidence for 1-AZA and 1-AMA binding near the microtubule colchicine site. (a) Polymerization of 10 $\mu$M tubulin with no ligand (black) and in the presence of 14 $\mu$M 1-AMA (red), 1-AZA (blue), 1-AZA plus UVA (cyan), and colchicine (purple) under polymerizing conditions (10% glycerol and 2 mM GTP) at 37 °C, monitoring absorbance at 450 nm. Error bars represent standard error of three separate trials. (b) Residues on photolabeled bovine tubulin peptides are conserved with tadpoles. Red amino acids were modified with 1-AZA, and spectra are shown in Figure S4. (c) Location of modified residues in bovine tubulin colchicine site. Tubulin $\beta$-2B is pale green, and tubulin $\alpha$-1D is brown. GTP is shown as gray spheres, and colchicine is shown as red sticks. Labeled amino acids are also shown as sticks: tubulin-$\beta$2/$\beta$3 I368 (blue), tubulin-$\beta$5 T366 (magenta), and tubulin-$\alpha$1D W406 (orange). Amino acids are numbered according to the sequences in Table S1, and the

**Figure** 3. continued

structure is adapted from PDB 1sa0 with the stathmin-like domain of RB3 removed for clarity. (d) Competition between 1-AZA and colchicine for binding/covalent addition to tubulin. Tubulin (15 $\mu$M) preincubated with 20 $\mu$M colchicine for 10 min before 8 $\mu$M 1-AZA addition (cyan). 15 $\mu$M tubulin with 8 $\mu$M 1-AZA (blue), and 8 $\mu$M 1-AZA by itself (black). All samples were photolyzed for 1.5 min with excitation at 400 nm. (e) Competition between 1-AMA and colchicine for binding to tubulin. 100 $\mu$M tubulin incubated with 50 $\mu$M 1-AMA for 10 min. Colchicine (5−645 $\mu$M) was then titrated with excitation at 425 nm.

8 to 16 $\mu$M (Figure 4b). Under these conditions only 22% of tadpoles were immobilized with 1-AMA in the presence of 2 $\mu$M EpoD ($n$ = 18, [1-AMA] = 9.9 ± 5.5 $\mu$M), compared to 61% of tadpoles without EpoD ($n$ = 17, [1-AMA] = 9.7 ± 3.7 $\mu$M) (Figure 4c). Another tubulin stabilizer, disco, was tested under the same conditions and gave similar results (Figure S8). Only 18% of tadpoles ($n$ = 27) were immobilized with 2 $\mu$M disco and 12.1 ± 3.0 $\mu$M AMA present. For 1-AZA, only 34% of tadpoles preincubated with EpoD were immobilized ($n$ = 23, [1-AZA] = 7.6 ± 2.0 $\mu$M), compared to 63% without EpoD ($n$ = 16, [1-AZA] = 4.6 ± 1.7 $\mu$M). Tadpoles incubated with 1-AZA for 30 min were photolyzed for 20 s with near-UV laser irradiation focused on the forebrain. EpoD prevented immobility (and increased survival) in tadpoles equilibrated and locally photolabeled with 1-AZA, suggesting a conserved "protective" effect against anthracene-induced immobility (Table 1).

To investigate further the anesthetic significance of the neuronal tubulin target, we incubated stage 40−47 tadpoles with allopregnanolone (3 $\mu$M, 5 trials, total $n$ = 47; or 4 $\mu$M, 4 trials, total $n$ = 41) in pond water with 0.5% ethanol for 3 h. The experiment was also performed with tadpoles preincubated for 1 h with 2 $\mu$M EpoD, then treated with allopregnanolone (3 $\mu$M, 5 trials, total $n$ = 50; or 4 $\mu$M, 4 trials, total $n$ = 42) in pond water for 3 h. As shown in Figure 5 and evaluated by $t$ test, EpoD decreased the percentage of tadpoles immobilized by allopregnanolone (at 3 $\mu$M, $P(T \leq t)$ two-tail = 0.036; at 4 $\mu$M, $P(T \leq t)$ two-tail = 0.179).

## ■ DISCUSSION

We have demonstrated the binding of 1-AMA and the photoactive analogue 1-AZA to a destabilizing site on neuronal tubulin, and have related the functional consequence of this interaction to general anesthetic sensitivity. The combined in vivo and in vitro approaches suggest that alteration of microtubule polymerization dynamics by general anesthetics can change the effective concentrations of these drugs. Specifically, our data demonstrate that the anthracenes decrease microtubule stability, and that supplying EpoD or disco that increases microtubule stability antagonizes anthracene anesthesia.

Previous photolabeling studies have identified tubulins as binding partners of general anesthetics and their analogues;[37−39] this includes a photoactive neurosteroid that also binds in the tubulin-$\beta$ colchicine binding site (Figure S5c).[39] In addition, compounds structurally related to the anthracenes, such as anthracen-9-yl esters and substituted anthracen-9-ones, potently inhibit microtubule polymerization and compete with colchicine binding to tubulin.[40,41] Disruption of microtubule dynamics as a contributor to anesthetic hypnosis has been suggested previously;[42] however, biologic data supporting this concept have been sparse, while increasing attention has focused on tubulin in relation to general anesthetic "off-pathway" effects, particularly regarding microtubule binding to the protein tau.[43−46]

The lethality noticed in our 1-AZA experiments was anticipated. General anesthetics are the most lethal of all drugs that physicians use, with therapeutic ratios of 2−4. When combined with concentration-effect Hill slopes of 10−20,[42,47] changes in target occupancy of less than an order of magnitude can convert immobility into lethality. The rapid photolysis of 1-AZA ($\tau_{1/2} \ll 1$ min under in vivo labeling conditions) provides this increase in target occupancy by reducing 1-AZA off-rates to near zero, effectively increasing 1-AZA affinity by several orders of magnitude. Less photoactive molecules, such as aziP$m$, provide greater "occupancy tuning" to avoid this outcome.[16] Finally, protection from lethality by EpoD raises the interesting possibility that tubulin can be both a therapeutic and toxicity target, as is the case for both colchicine and taxol.

Our in vivo results with 1-AMA and EpoD provide strong evidence that destabilization of neuronal microtubules—important structural and transport proteins in the cell—provides a path to achieving general anesthesia. The high concentration and myriad functional roles of microtubules in neurons suggest that this is a common, and perhaps evolutionarily conserved anesthetic mechanism. Tubulin is an attractive target for mechanistic study because of a diverse and well-studied pharmacology circumventing the need for laborious genetic approaches. We have yet to test the contribution of the microtubule state to 1-AMA sensitivity in higher organisms; however, the development of microtubule stabilizing agents (including EpoD[48]) that cross the blood brain barrier allows investigation of tubulin dynamics in relation to other injectable and volatile anesthetics. One example is the large class of neurosteroids, some of which possess a phenanthrene core of structural similarity to the anthracene anesthetics, 1-AMA and 1-AZA. Several neurosteroids (e.g., alphaxolone, alphadolone, hydroxydione, minaxolone, allopregnanolone) have been employed as general anesthetics. A photoactive variant of allopregnanolone (6-azi-pregnanolone) was shown recently to bind tubulin and inhibit polymerization.[39] Also, an estradiol metabolite, 2-methoxyestradiol, of similar structure to allopregnanolone displayed a tubulin interaction. At high concentrations, it inhibited microtubule polymerization and acted as a weak inhibitor of colchicine-tubulin binding.[49] Finally, the neurosteroid pregnenolone was demonstrated to bind to microtubule-associated protein 2 (MAP2) and increase tubulin polymerization.[50] These observations motivated us to investigate whether EpoD (2 $\mu$M) would inhibit tadpole immobilization by a prototypal neurosteroid, allopregnanolone. At 3 $\mu$M allopregnanolone, these experiments replicated the 1-AMA-EpoD result (Figure 5).

However, conserved pharmacology is not ensured; the volatile anesthetic, halothane, for instance, has been shown to have little effect on microtubule polymerization in vitro, trending toward a stabilizing influence.[46] Our in vitro data with propofol and isoflurane (Figure S9) indicate that these smaller and clinically used general anesthetics also promote tubulin polymerization, much like taxol,[51] which is opposite the

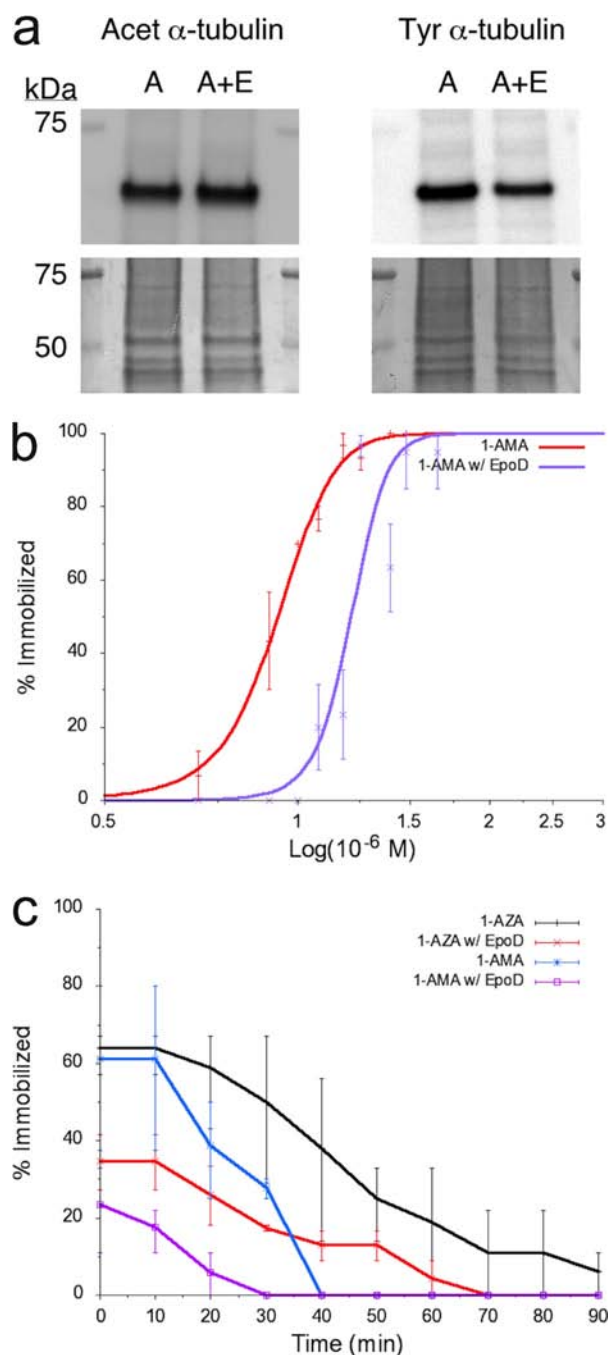**a** Acet α-tubulin    Tyr α-tubulin



**b**



**c**

**Figure 4.** EpoD efficacy via 5 μg Western blot, anesthetic dose–response curves and recovery kinetics. (a) Increased polymerization of microtubules by EpoD was confirmed in vivo by Western blotting for stabilized microtubule marker (acetylated α-tubulin) and soluble tubulin marker (tyrosinated α-tubulin). Coomassie stained membranes are shown below for loading control. (b) 1-AMA induction involving tadpole recovery after 30-min incubation with 2 μM EpoD and 1-AMA at varied concentrations (purple, $EC_{50}$ = 8 μM) compared with 1-AMA alone (red, $EC_{50}$ = 16 μM). (c) Time course for recovery of tadpoles after switching to pond water after 30-min incubation in the presence of 1-AZA with 2 μM EpoD (n = 23, 7.6 ± 2.0 μM, blue), 1-AZA alone (n = 16, 4.6 ± 1.7 μM, black), 1-AMA with 2 μM EpoD (n = 18, 9.9 ± 5.5 μM, purple), and 1-AMA alone (n = 17, 9.7 ± 3.7 μM, red). A range between two sets of tadpoles (each set half of total) is included for each trial.

effect of 1-AMA, 1-AZA, 6-azi-pregnanolone, and 2-methoxyestradiol. Thus, we believe that microtubule destabilization,
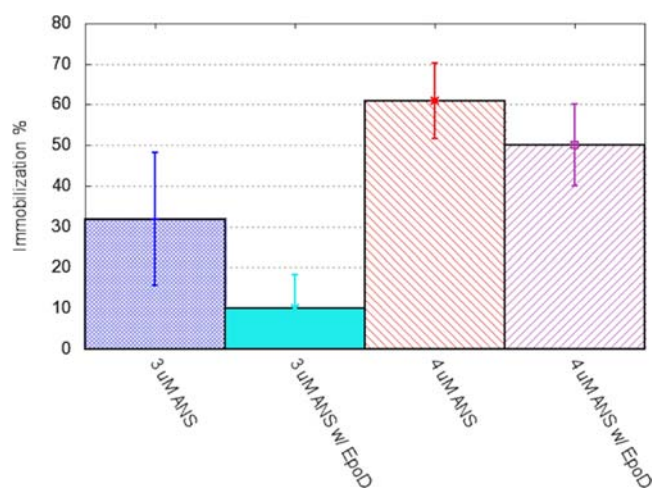


**Figure 5.** EpoD effect on neurosteroid allopregnanolone (ANS) dose response in tadpoles. EpoD (2 μM) lowered tadpole immobilization from 34 ± 20% to 10 ± 7% in the presence of 3 μM allopregnanolone (t test, $P(T \leq t)$ two-tail = 0.036) and from 61 ± 9% to 50 ± 10% (t test, $P(T \leq t)$ two-tail = 0.179) in the presence of 4 μM allopregnanolone after 3 h incubation in pond water with 0.5% ethanol, before switching to fresh water.

per se, may not be a unitary mechanism for achieving general anesthesia. It is likely that microtubule dynamics are dependent on optimal tubulin stabilization, and that anesthetics may destabilize in either direction.

Indirect pharmacological effects on the anesthetic state may also plausibly arise from microtubule status, based on the important role of microtubules in supporting the trafficking of membrane proteins to the neuron cell surface, as well as providing a scaffold for functional ion channels such as the GABA and NMDA receptors.[52−55] Microtubule status is intricately linked to the complement of transmembrane proteins found at the cell surface and can impact physiological ion transport.[56] In this context, we hypothesize that destabilization of neuronal microtubules by 1-AMA may also deactivate many important transmembrane proteins (e.g., ligand-gated ion channels) that are important in maintaining mobility. The finding that EpoD can also counteract immobilization with allopregnanolone in tadpoles increases the potential significance of the neuronal tubulin target to clinical anesthesia. In this light, it should also be considered whether the modulation of neuronal microtubule status by common cancer therapeutics may positively or negatively impact the efficacy of general anesthetics.

## ■ CONCLUSION

This study provides a critical first piece of the puzzle in understanding the mechanism by which two anthracene anesthetics, 1-AMA and 1-AZA, achieve immobilization in tadpoles and other vertebrate model organisms. Although tubulin had been shown previously to bind various anesthetics, and various tubulin roles in general anesthesia have been postulated, this study provides the first evidence of a neuronal tubulin functional role in maintaining the anesthetic state. The important role of microtubule status in effecting general anesthesia was validated using two small molecule drugs, EpoD and disco. Our finding that both 1-AMA and allopregnanolone activity in tadpoles can be modulated by EpoD increases the likelihood that neuronal tubulin contributes

to the state of general anesthesia. Distinctively, this study provides a new validated anesthetic target protein, which creates new opportunities for mechanistic study and drug discovery. Furthermore, 1-AZA has broad utility as a "caged" anesthetic. An increase in fluorescence intensity upon photo-activation serves to identify the labeled site(s). The identification of beta-tubulin and other proteins as 1-AZA-labeled targets highlights the important roles now played by anesthetic probe molecules. The use of such probes in optoanesthetic research will bring even greater spatial and temporal resolution to explorations of this important biomedical frontier.

## ASSOCIATED CONTENT

### Supporting Information
Supplementary Figures S1−S9 and Table S1. This material is available free of charge via the Internet at http://pubs.acs.org.

## AUTHOR INFORMATION

### Corresponding Author
ivandmo@sas.upenn.edu; roderic.eckenhoff@uphs.upenn.edu
### Author Contributions
§D.J.E. and B.P.W. contributed equally to this work.
### Notes
The authors declare no competing financial interest.

## ACKNOWLEDGMENTS

## REFERENCES

(1) Eckenhoff, R. G.; Johansson, J. S. Pharmacol. Rev. 1997, 49, 343−368.
(2) Bhattacharya, A. A.; Curry, S.; Franks, N. P. J. Biol. Chem. 2000, 275, 38731−38738.
(3) Johansson, J. S.; Manderson, G. A.; Ramoni, R.; Grolli, S.; Eckenhoff, R. G. FEBS J. 2005, 272, 573−581.
(4) Vedula, L. S.; Brannigan, G.; Economou, N. J.; Xi, J.; Hall, M. A.; Liu, R.; Rossi, M. J.; Dailey, W. P.; Grasty, K. C.; Klein, M. L.; Eckenhoff, R. G.; Loll, P. J. J. Biol. Chem. 2009, 284, 24176−24184.
(5) Stein, M.; Middendorp, S. J.; Carta, V.; Pejo, E.; Raines, D. E.; Forman, S. A.; Sigel, E.; Trauner, D. Angew. Chem., Int. Ed. 2012, 51, 10500−10504.
(6) Eckenhoff, R. G.; Knoll, F. J.; Greenblatt, E. P.; Dailey, W. P. J. Med. Chem. 2002, 45, 1879−1886.
(7) Husain, S. S.; Ziebell, M. R.; Ruesch, D.; Hong, F.; Arevalo, E.; Kosterlitz, J. A.; Olsen, R. W.; Forman, S. A.; Cohen, J. B.; Miller, K. W. J. Med. Chem. 2003, 46, 1257−1265.
(8) Bright, D. P.; Adham, S. D.; Lemaire, L. C. J. M.; Benavides, R.; Gruss, M.; Taylor, G. W.; Smith, E. H.; Franks, N. P. J. Biol. Chem. 2007, 282, 12038−12047.
(9) Eckenhoff, R. G.; Xi, J.; Shimaoka, M.; Bhattacharji, A.; Covarrubias, M.; Dailey, W. P. ACS Chem. Neurosci. 2010, 1, 139−145.
(10) Hall, M. A.; Xi, J.; Lor, C.; Dai, S.; Pearce, R.; Dailey, W. P.; Eckenhoff, R. G. J. Med. Chem. 2010, 53, 5667−5675.
(11) Stewart, D. S.; Savechenkov, P. Y.; Dostalova, Z.; Chiara, D. C.; Ge, R.; Raines, D. E.; Cohen, J. B.; Forman, S. A.; Bruzik, K. S.; Miller, K. W. J. Med. Chem. 2011, 54, 8124−8135.
(12) Chiara, D. C.; Dangott, L. J.; Eckenhoff, R. G.; Cohen, J. B. Biochemistry 2003, 42, 13457−13467.
(13) Li, G.-D.; Chiara, D. C.; Sawyer, G. W.; Husain, S. S.; Olsen, R. W.; Cohen, J. B. J. Neurosci. 2006, 26, 11599−11605.
(14) Butts, C. A.; Xi, J.; Brannigan, G.; Saad, A. A.; Venkatachalan, S. P.; Pearce, R. A.; Klein, M. L.; Eckenhoff, R. G.; Dmochowski, I. J. Proc. Natl. Acad. Sci. U.S.A. 2009, 106, 6501−6506.
(15) Emerson, D. J.; Liao, Z.; Eckenhoff, R. G.; Dmochowski, I. J. Anesthesiology 2012, 116, 1363.
(16) Weiser, B. P.; Kelz, M. B.; Eckenhoff, R. G. J. Biol. Chem. 2013, 288, 1279−1285.
(17) Wittmer, L. L.; Hu, Y.; Kalkbrenner, M.; Evers, A. S.; Zorumski, C. F.; Covey, D. F. Mol. Pharmacol. 1996, 50, 1581−1586.
(18) The PyMOL Molecular Graphics System, Version 1.5.0.4; Schrödinger, LLC.
(19) Tubulin Polymerization Assay Kit. www.cytoskeleton.com/pdf-storage/datasheets/BK006P.pdf (accessed Feb 11, 2013).
(20) Paolini, S.; Scaloni, A.; Amoresano, A.; Marchese, S.; Napolitano, E.; Pelosi, P. Chem. Senses 1998, 23, 689−698.
(21) Lehman, P.; Berry, R. J. Am. Chem. Soc. 1973, 95, 8614−8620.
(22) Geiger, M. W.; Elliot, M. M.; Karacostas, V. D.; Moricone, T. J.; Salmon, J. B.; Sideli, V. L.; Onge, M. A. S. Photochem. Photobiol. 1984, 40, 545−548.
(23) Cheng, T.; Zhao, Y.; Li, X.; Lin, F.; Xu, Y.; Zhang, X.; Li, Y.; Wang, R.; Lai, L. J. Chem. Inf. Modell. 2007, 47, 2140−2148.
(24) Xie, F.; Sivakumar, K.; Zeng, Q.; Bruckman, M. A.; Hodges, B.; Wang, Q. Tetrahedron 2008, 64, 2906−2914.
(25) Harris, R. F.; Nation, A. J.; Copeland, G. T.; Miller, S. J. J. Am. Chem. Soc. 2000, 122, 11270−11271.
(26) Li, X.; Zhang, G.; Ma, H.; Zhang, D.; Li, J.; Zhu, D. J. Am. Chem. Soc. 2004, 126, 11543−11548.
(27) Yang, W.; Fan, H.; Gao, X.; Gao, S.; Karnati, V. V. R.; Ni, W.; Hooks, W. B.; Carson, J.; Weston, B.; Wang, B. Chem. Biol. 2004, 11, 439−448.
(28) Magri, D. C.; Brown, G. J.; McClean, G. D.; De Silva, A. P. J. Am. Chem. Soc. 2006, 128, 4950−4951.
(29) Chang, K.-C.; Su, I.-H.; Senthilvelan, A.; Chung, W.-S. Org. Lett. 2007, 9, 3363−3366.
(30) Ravelli, R. B. G.; Gigant, B.; Curmi, P. A.; Jourdain, I; Lachkar, S.; Sobel, A.; Knossow, M. Nature 2004, 428, 198−202.
(31) Dorleans, A.; Gigant, B.; Ravelli, R. B. G.; Mailliet, P.; Mikol, V.; Knossow, M. Proc. Natl. Acad. Sci. U.S.A. 2009, 106, 13775−13779.
(32) Malkin, J. Photophysical and Photochemical Properties of Aromatic Compounds, 1st ed.; CRC Press: Boca Raton, FL, 1992.
(33) Ballatore, C.; Brunden, K. R.; Huryn, D. M.; Trojanowski, J. Q.; Lee, V. M.-Y.; Smith, A. B., III J. Med. Chem. 2012, 55, 8979−8996.
(34) Nettles, J. H.; Li, H.; Cornett, B.; Krahn, J. M.; Snyder, J. P.; Downing, K. H. Science 2004, 305, 866−869.
(35) Brunden, K. R.; Yao, Y.; Potuzak, J. S.; Ferrer, N. I.; Ballatore, C.; James, M. J.; Hogan, A.-M. L.; Trojanowski, J. Q.; Smith, A. B.; Lee, V. M.-Y. Pharmacol. Res. 2011, 63, 341−351.
(36) Janke, C.; Chloë Bulinski, J. Nat. Rev. Mol. Cell Biol. 2011, 12, 773−786.
(37) Xi, J.; Liu, R.; Asbury, G. R.; Eckenhoff, M. F.; Eckenhoff, R. G. J. Biol. Chem. 2004, 279, 19628−19633.
(38) Pan, J. Z.; Xi, J.; Tobias, J. W.; Eckenhoff, M. F.; Eckenhoff, R. G. J. Proteome Res. 2007, 6, 582−592.
(39) Chen, Z.-W.; Chen, L.-H.; Akentieva, N.; Lichti, C. F.; Darbandi, R.; Hastings, R.; Covey, D. F.; Reichert, D. E.; Townsend, R. R.; Evers, A. S. Electrophoresis 2012, 33, 666−674.
(40) Zuse, A.; Schmidt, P.; Baasner, S.; Böhm, K. J.; Müller, K.; Gerlach, M.; Günther, E. G.; Unger, E.; Prinz, H. J. Med. Chem. 2007, 50, 6059−6066.
(41) Prinz, H.; Schmidt, P.; Böhm, K. J.; Baasner, S.; Müller, K.; Unger, E.; Gerlach, M.; Günther, E. G. J. Med. Chem. 2009, 52, 1284−1294.

(42) Hameroff, S.; Nip, A.; Porter, M.; Tuszynski, J. *BioSystems* **2002**, *64*, 149−168.

(43) Tang, J. X.; Eckenhoff, M. F.; Eckenhoff, R. G. *Curr. Opin. Anaesthesiol.* **2011**, *24*, 389−394.

(44) Le Freche, H.; Brouillette, J.; Fernandez-Gomez, F.-J.; Patin, P.; Caillierez, R.; Zommer, N.; Sergeant, N.; Buée-Scherrer, V.; Lebuffe, G.; Blum, D.; Buée, L. *Anesthesiology* **2012**, *116*, 779−787.

(45) Whittington, R.; Marcouiller, F.; Papon, M.; Julien, C.; Morin, F.; Emala, C.; Planel, E. *PLoS ONE* **2011**, *6*, e16648.

(46) Craddock, T. J. A.; St. George, M.; Freedman, H.; Barakat, K. H.; Damaraju, S.; Hameroff, S.; Tuszynski, J. A. *PLoS ONE* **2012**, *7*, e37251.

(47) Friedman, E. B.; Sun, Y.; Moore, J. T.; Hung, H.-T.; Meng, Q. C.; Perera, P.; Joiner, W. J.; Thomas, S. A.; Eckenhoff, R. G.; Sehgal, A.; Kelz, M. B. *PLoS ONE* **2010**, *5*, e11903.

(48) Brunden, K. R.; Ballatore, C.; Lee, V. M. -Y.; Smith, A. B.; Trojanowski, J. Q. *Biochem. Soc. Trans.* **2012**, *40*, 661−666.

(49) D'Amato, R. J.; Lin, C. M.; Flynn, E.; Folkman, J.; Hamel, E. *Proc. Natl. Acad. Sci. U.S.A.* **1994**, *91*, 3964−3968.

(50) Murakami, K.; Fellous, A.; Baulieu, E.-E.; Robel, P. *Proc. Natl. Acad. Sci. U.S.A.* **2000**, *97*, 3579−3584.

(51) Wani, M. C.; Taylor, H. L.; Wall, M. E.; Coggon, P.; McPhail, A. T. *J. Am. Chem. Soc.* **1971**, *93*, 2325−2327.

(52) Passafaro, M.; Sheng, M. *Curr. Biol.* **1999**, *9*, R261−263.

(53) Wang, H.; Olsen, R. W. *J. Neurochem.* **2002**, *75*, 644−655.

(54) Eriksson, M.; Samuelsson, H.; Björklund, S.; Tortosa, E.; Avila, J.; Samuelsson, E.-B.; Benedikz, E.; Sundström, E. *Neurosci. Lett.* **2010**, *475*, 33−37.

(55) Kapitein, L. C.; Yau, K. W.; Gouveia, S. M.; Van der Zwan, W. A.; Wulf, P. S.; Keijzer, N.; Demmers, J.; Jaworski, J.; Akhmanova, A.; Hoogenraad, C. C. *J. Neurosci.* **2011**, *31*, 8194−8209.

(56) Lei, P.; Ayton, S.; Finkelstein, D. I.; Spoerri, L.; Ciccotosto, G. D.; Wright, D. K.; Wong, B. X. W.; Adlard, P. A.; Cherny, R. A.; Lam, L. Q.; Roberts, B. R.; Volitakis, I.; Egan, G. F.; McLean, C. A.; Cappai, R.; Duce, J. A.; Bush, A. I. *Nat. Med.* **2012**, *18*, 291−295.

5398

dx.doi.org/10.1021/ja311171u | *J. Am. Chem. Soc.* 2013, 135, 5389−5398